Neurobiology of Disease 164 (2022) 105631

Contents lists available at ScienceDirect

Neurobiology of Disease

journal homepage: www.elsevier.com/locate/ynbdi

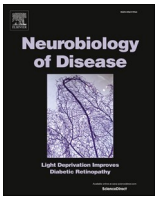

Human apolipoprotein E isoforms are differentially sialylated and the sialic acid moiety in ApoE2 attenuates ApoE2-Aβ interaction and Aβ fibrillation

Hee-Jung Moon [a], Vahram Haroutunian [c], Liqin Zhao [a,b,*]

[a] Department of Pharmacology and Toxicology, School of Pharmacy, University of Kansas, Lawrence, KS 66045, USA
[b] Neuroscience Graduate Program, University of Kansas, Lawrence, KS 66045, USA
[c] The Alzheimer's Disease Research Center, Icahn School of Medicine at Mount Sinai, New York, NY 100029, USA

ARTICLE INFO

Keywords:
Late-onset Alzheimer's disease (LOAD)
Apolipoprotein E (ApoE)
Amyloid-β (Aβ)
ApoE-Aβ interaction
Sialic acid
Sialylation

ABSTRACT

The *APOE* genotype is the most prominent genetic risk factor for the development of late-onset Alzheimer''s disease (LOAD); however, the underlying mechanisms remain unclear. In the present study, we found that the sialylation profiles of ApoE protein in the human brain are significantly different among the three isoforms, with ApoE2 exhibiting the most abundant sialic acid modification whereas ApoE4 had the least. We further observed that the sialic acid moiety in ApoE2 significantly affected the interaction between ApoE2 and Aβ peptides. The removal of sialic acid in ApoE2 increased the ApoE2 binding affinity for the Aβ17–24 region of Aβ and promoted Aβ fibrillation. These findings provide a plausible explanation for the well-documented differential roles of ApoE isoforms in Aβ pathogenesis. Specifically, compared to the other two isotypes, the higher expression of sialic acid in ApoE2 may contribute to the less potent interaction between ApoE2 and Aβ and ultimately the slower rate of brain Aβ deposition, a mechanism thought to underlie ApoE2-mediated decreased risk for AD. Future studies are warranted to determine whether the differential sialylation in ApoE isoforms may also contribute to some of their other distinct properties, such as their divergent preferences in associations with lipids and lipoproteins, as well as their potential impact on neuroinflammation through modulation of microglial Siglec activity. Overall, our findings lead to the insight that the sialic acid structure is an important posttranslational modification (PTM) that alters ApoE protein functions with relevance for AD.

1. Introduction

Glycosylation is an important posttranslational modification (PTM) that significantly affects the biological properties of proteins. Glycan is a crucial structure that modulates protein folding, stability, protein-protein interaction, and cellular signaling. Sialylation, a part of glycosylation, occurs when sialic acid is attached to specific terminal positions on glycoproteins and glycolipids (Schedin-Weiss et al., 2014; Stanley, 2011). Sialic acid, a 9-carbon backbone sugar molecule with a negative charge and high hydrophilicity, is one of the most abundant terminal monosaccharides expressed on glycoconjugates of the eukaryotic cell surface (Keppler et al., 1999; Yoo et al., 2015). *N*-acetylneuraminic acid (2-keto-5-acetamido-3,5-dideoxy-*D*-glycero-*D*-galactononulosonic acid; Neu5Ac) is the most common form of sialic acid present in human glycoconjugates, including glycoproteins, gangliosides, glycosaminoglycans, and mucins. Sialic acid is widely distributed in the human body, with the highest concentration found in the central nervous system (CNS). Neural cell membranes contain approximately 20-fold more sialic acid than other types of cellular membranes, supporting that sialic acid plays a unique structural and functional role in brain development, regeneration, and learning (Hayakawa and Varki, 2012; Yoo et al., 2015).

Apolipoprotein E (ApoE), a 34 kDa glycoprotein consisting of 299 amino acids (aa), is involved in cholesterol transport and metabolism as a surface component of lipoprotein particles (Huang and Mahley, 2014; Yu et al., 2014). The ApoE protein structure comprises two functional

Abbreviations: Aβ, amyloid-β; AD, Alzheimer's disease; ApoE, apolipoprotein E; CNS, central nervous system; CSF, cerebrospinal fluid; HBP, hexosamine biosynthetic pathway; HDL, high-density lipoprotein; HK, hexokinase; LDL-R, low-density lipoprotein receptor; LOAD, late-onset Alzheimer's disease; MW, molecular weight; Neu5Ac, *N*-acetylneuraminic acid (2-keto-5-acetamido-3,5-dideoxy-D-glycero-D-galactononulosonic acid); PTM, posttranslational modification; rhApoE2, recombinant human ApoE2; ThT, thioflavin T; UDP-GlcNAc, 5′-diphosphate-*N*-acetyl-D-glucosamine; VLDL, very-low-density lipoprotein.

* Corresponding author at: Department of Pharmacology and Toxicology, University of Kansas, 1251 Wescoe Hall Dr., Lawrence, KS 66045, USA.
E-mail address: lzhao@ku.edu (L. Zhao).

https://doi.org/10.1016/j.nbd.2022.105631
Received 24 June 2021; Received in revised form 9 January 2022; Accepted 11 January 2022
Available online 15 January 2022

domains connected through a hinge region: an amino-terminal (N-terminal) domain containing a highly positively charged receptor-binding region and a carboxyl-terminal (C-terminal) domain including a lipid-binding region. ApoE is synthesized and secreted by many cell types, including hepatocytes, smooth muscle cells, neural cells, and macrophages (Hatters et al., 2006; Hauser et al., 2011). In the periphery, ApoE plays essential roles in very-low-density lipoprotein (VLDL) remnant clearance, immune response, cell proliferation, and lymphocyte activation. In the CNS, ApoE is mainly produced by astrocytes and, to a lesser extent, microglia as the major apolipoprotein constituent of high-density lipoprotein (HDL)-like particles (Bu, 2009; Mahley, 2016; Mahley et al., 2009). Although brain ApoE is primarily derived from astrocytes, neurons can also synthesize ApoE as observed in both human and mouse brains (Harris et al., 2004; Tesseur et al., 2000; Xu et al., 1999). In fact, neuron-derived ApoE is reported to contribute to approximately 20% of total ApoE protein in the CNS (Knoferle et al., 2014). Studies have also shown that neuronal expression of ApoE is increased under stress and after injuries (Aoki et al., 2003; Xu et al., 2006). ApoE proteins are highly glycosylated, and because ApoE does not contain the consensus sequence for *N*-glycan (Asn-*X*-Ser/Thr), carbohydrate moieties are attached to ApoE through an *O*-linkage on Ser/Thr residues (Flowers et al., 2020; Halim et al., 2013; Kawasaki et al., 2009; Lee et al., 2010). LC-MS/MS characterization studies have predicted a total of 7 *O*-linked glycosylation residues (Thr8, Thr18, Thr194, Ser197, Thr289, Ser290, and Ser296) in human ApoE protein (Flowers et al., 2020; Halim et al., 2013; Lee et al., 2010). Moreover, studies have indicated that human ApoE protein in the cerebrospinal fluid (CSF) are more extensively sialylated than plasma ApoE (Halim et al., 2013).

Human ApoE exists as three major isoforms (ApoE2, ApoE3, and ApoE4), with ApoE4 imposing the highest genetic risk for the development of late-onset Alzheimer's disease (LOAD) and ApoE2 providing neuroprotection against LOAD (Hatters et al., 2006; Huang and Mahley, 2014; Huynh et al., 2017; Liu et al., 2013; Wu and Zhao, 2016). Though it is a fact that human ApoE isoforms confer a drastically distinct impact on the incidence of AD, it remains unclear how the structural and biological properties of ApoE contribute to its pathogenic role in the development of LOAD. The three ApoE isoforms differ by just two amino acid substitutions at residues 112 and 158: ApoE2 (Cys112, Cys158), ApoE3 (Cys112, Arg158), and ApoE4 (Arg112, Arg158). However, these minor differences may confer a considerable impact on the three-dimensional structure of ApoE isoproteins, which may alter the binding ability of ApoE protein to lipids, low-density lipoprotein receptors (LDL-R), and Aβ (Hatters et al., 2006; Huang and Mahley, 2014; Zhong and Weisgraber, 2009).

A crucial feature of AD pathology is the formation of Aβ oligomers and plaques (Aleshkov et al., 1997; Bentley et al., 2002; Verghese et al., 2013). Even though the role of Aβ in AD development is still debated, Aβ represents one of the main components of AD pathogenesis. Many studies have demonstrated that ApoE interacts with Aβ in an isoform-specific manner and that the ApoE-Aβ complex contributes to Aβ aggregation and plaque formation, which consequently facilitates disease progression (LaDu et al., 1994; Manelli et al., 2004; Zhou et al., 1996). In particular, ApoE4 has been shown to enhance Aβ oligomerization, whereas ApoE2 has been associated with a slower rate of brain Aβ deposition (Manelli et al., 2004; Tai et al., 2013). While recent studies have attempted to elucidate the association between ApoE and Aβ and how this association might contribute to Aβ pathogenesis (Huynh et al., 2017; Wisniewski and Drummond, 2020), the mechanism by which ApoE protein variants differentially interact with Aβ remains unclear.

Our previous work demonstrated that neural cells transfected with human ApoE isoforms exhibited distinct patterns in ApoE protein expression, with more immunoreactive ApoE bands detected in cells transfected with ApoE2. In the present study, the PTM expression profiles of the three ApoE isoforms were examined in postmortem human brain tissues and neural cell lines with a specific emphasis on ApoE protein sialylation. Our analyses revealed distinctive differences in sialylation profiles among the three ApoE isoproteins. Furthermore, the data indicated that ApoE sialylation significantly reduced ApoE-Aβ interaction and Aβ fibrillation, Collectively, these novel findings point to a potentially crucial role of the sialic acid moiety expressed on human ApoE protein in the development of Aβ pathology associated with AD.

2. Materials and methods

2.1. Materials

Unless stated otherwise, all chemicals and reagents were purchased from Sigma-Aldrich (St. Louis, MO). Human brain cerebral cortex whole tissue lysate (adult whole normal; Cat. #NB820–59182)] was purchase from Novus (Centennial, CO). The Aβ1–16 (Cat. #H-2958), Aβ12–28 (Cat. #H-7910), Aβ25–35 (Cat. #H-1192), Aβ1–40 (Cat. #H-5568), and Aβ1–42 (Cat. #H-1368) peptides were purchased from BACHEM (Torrance, CA). Recombinant human ApoE2 (source: *E. coli*; Cat. #350–12) was purchased from PeproTech (Rocky Hill, NJ) and reconstituted in 20 mM sodium phosphate (pH 7.8) to a concentration of 1 mg/mL.

2.2. Human brain tissue protein extraction

Human brain tissues were obtained from the Mount Sinai/JJ Peters VA Medical Center NIH Brain and Tissue Repository (NBTR) through the NIH NeuroBioBank. All tissues were derived from the inferior frontal cortex (Brodmann area 47) of subjects free of AD or related dementia ($n = 2$ per *APOE* genotype, age 57–72). 15 mg of frozen pulverized tissue samples were sonicated in 500 μL of tissue protein extraction reagent (TPER, Life Technologices, Cat. #78510) supplemented with protease and phosphatase inhibitors (Thermo, Cat. #A32961). Homogenates were centrifuged at 10,000*g* × 10 min, and the supernatants were collected. Total protein concentration was determined by using a BCA Protein Assay Kit (Thermo, Cat. #23227).

2.3. Cell lines

Human neuroblastoma cell line SH-SY5Y cells (ATCC CRL-2266) were purchased from ATCC (Manassas, VA) and maintained in Dulbecco's modified eagle's medium (DMEM) high glucose (Gibco, Cat. #11-965-118) supplemented with 10% fetal bovine serum (FBS) and 1% penicillin/streptomycin at 37 °C in a humidified 5% CO_2. Cells below passage 12 and in the exponential growth phase were used in all experiments.

2.4. Transfection

pCMV6-human ApoE2, ApoE3, and ApoE4 have been used as previously described (Wu et al., 2018). The threonine residue at the *Mlu* I site of the plasmids was mutated to alanine to eliminate a consensus sequence of *N*-glycan. Transfections were performed at 60% cell confluence using jetPRIME reagent (Polyplus Transfection, Cat. #114-07). Cells were transfected with 2 μg of DNA in 6-well plate for 48 h before protein expression analysis and further experiments. The culture media were harvested at the same time with protease and phosphatase inhibitor cocktail and centrifuged at 10,000*g* × 5 min to eliminate cell debris. The media fractions were subjected to SDS-PAGE for protein analysis.

2.5. Enzymatic deglycosylation

Deglycosylation was achieved using PNGase F (NEB Cat. #P0704), Endo H (NEB, Cat. #P0702), *O*-glycosidase (NEB Cat. #P0733), and α2–3,6,8,9 neuraminidase A (NEB, Cat. #P0722) according to the manufacturer's instructions. 20 μg of total protein sample was denatured by incubation with glycoprotein denaturing buffer for 10 min at 95 °C. Denatured protein samples were treated with glycosidase enzyme in

GlycoBuffer for 1 h at 37 °C. For α2–3,6,8,9 neuraminidase A treatment, 20 μg of total protein sample or 3 μL of media fraction was incubated with 20 units of the enzyme in a final volume of 10 μL for 1 h at 37 °C. The reaction was stopped by mixing with Laemmli sample buffer containing β-mercaptoethanol and analyzed by Western blot.

2.6. Generation of expression constructs

The Strep-tag II sequence was engineered at the 3′ end of human ApoE2 by first subcloning the gene into the pEXPR-IBA42 vector containing Strep-tag II, using the following primer pair: ApoE_*Nhe*I_forward [5′-GACGGCTAGCATGAAGGTTC TGTGGGCT-3′ (NheI restriction site is underlined)] and ApoE_BsaI_reverse (5′-GCGCTGAGA CCGTGATTGTCGCTGGGCAC-3′). The hApoE2-StrepII DNA was amplified by PCR from pEXPR-IBA42_hApoE2 plasmid using the following primer pair: ApoE_NheI_forward and strep tag_*Hin*dIII_reverse [5′-ACT-TAAGCTTATTATTTTTCGAACTGCG-3′ (HindIII restriction site is underlined)]. The human ApoE2-StrepII-tagged DNA was then lifted out by PCR and cloned into pcDNA3.1(-) expression vector at the NheI and HindIII sites. Sequences were verified by DNA sequencing (Genewiz, South Plainfield, NJ).

2.7. Production and purification of rhApoE2

Recombinant human ApoE2 was produced in HEK293 cells (FreeStyle 293-F cells, Thermo Fisher Scientific). Briefly, 293-F cells in FreeStyle 293 expression medium were transfected with pcDNA3.1 (-—)-hApoE2-Strep II (a mammalian expression vector for the human ApoE2 with C-terminal fused with a Strep II-tag) using 293fectin transfection reagent according to the manufacturer's protocol. After 96 h of incubation on an orbital shaker (125 rpm) at 37 °C with 8% CO2, the culture medium was collected by centrifugation and concentrated using a 10 kDa molecular weight cutoff (MWCO) filter. The hApoE2 was then purified using a Strep-Tactin affinity chromatography following the kit (iba, Cat. #2-—5998-000) protocol. SDS-PAGE and Western blot analysis examined the purity of the isolated proteins. Protein concentrations were determined by a Pierce BCA protein assay kit. Typical yields were 30–35 mg of protein per liter of culture.

2.8. Myc pull-down assay

For pull-down reaction, 20 μL of Myc-Trap agarose beads (chromoteck, Cat. #yta-10) were incubated for 1 h at 4 °C with 100 μL of the cultured medium from SH-SY5Y cells expressing human ApoE2, ApoE3, and ApoE4 protein. The beads were washed with washing buffer (25 mM Tris, 150 mM NaCl, 1 mM EDTA, 1% NP-40, 5% glycerol, pH 7.4) three times and boiled in Laemmli loading buffer. Proteins were further analyzed by SDS-PAGE/immunoblotting.

2.9. Immunoblotting

Protein extracts were separated by SDS-PAGE and probed with respective antibodies. Briefly, 10–30 μg of total protein sample isolated from tissue, cells, or 1–5 μL of media fraction was resolved via reducing SDS-PAGE. Resolved proteins were then transferred to PVDF membranes and blocked with blocking buffer. Membranes were incubated with customized dilutions of the indicated primary antibodies followed by incubation with an appropriate HRP-conjugated secondary antibody at RT for 1 h. Bands were visualized using chemiluminescence with an ECL detection kit (BioRad, Cat. #1705061) and scanned using the C-Digit Blot Scanner (LI-COR). Antibodies used were human ApoE (Millipore, Cat. #178479), mouse ApoE (Biolegend, Cat. #674802), anti-myc (Origene, Cat. #TA150081), Aβ (6e10, Biolegend, Cat. #803001), Aβ (4g8, Biolegend, Cat. #800701), Aβ (22–35, Sigma, Cat. #A3356), and β-tubulin (Pierce, Cat. #MA5–11732).

2.10. ApoE-Aβ complex formation and detection

For a typical binding reaction, it was performed following the method described previously (Aleshkov et al., 1997). Briefly, 0.9 μg of rhApoE2 was mixed with 1 μL of 1 M Tris HCl buffer (pH 7.4) and 3.4 μL of 1 mM Aβ peptide solution in a total volume of 34 μL and incubated at 37 °C for 2 h. The reactions were stopped by adding 4× Laemmli buffer without β-mercaptoethanol, boiled for 5 min, and separated on 12.5% SDS-PAGE. Separated complexes then proceeded to immunoblotting analysis as described above.

2.11. ApoE-Aβ complex immunoprecipitation

Immunoprecipitation of ApoE-Aβ complexes were performed using a Pierce Co-IP kit (Thermo, Cat. #26149), following the manufacturer's instructions. Briefly, anti-human monoclonal Aβ antibody (6e10) was coupled to AminoLink Plus coupling resin. ApoE-Aβ complexes were prepared as indicated above. Each complex preparation was incubated with 6e10-conjugated agarose resin for 90 min at 4 °C, followed by three washes with IP lysis/wash buffer. The bound complexes were eluted using elution buffer. Upon IP, ApoE was detected by immunoblotting using goat polyclonal ApoE antibody.

2.12. Aβ1–42 aggregation assay

The Aβ1–42 aggregation assay was performed using SensoLyte Thioflavin T (ThT) Aβ1–42 aggregation kit (fluorometric) in a cell-free system (Anaspec, Cat. #AS-72214), according to the manufacturer's instructions. For α2–3,6,8,9 neuraminidase A treatment, 0.5 μg of rhApoE2 protein was incubated with 20 units of the enzyme in a final volume of 10 μL for 10 min at 37 °C. To measure Aβ1–42 fibril formation in 96-well black non-binding microplate (Fisher, Cat. #07–000-634), 10 μL of 2 mM ThT and 5 μL of sialyalted_rhApoE2 or desialylated_rhApoE2 were added into each well and mixed with 85 μL of Aβ 1–42 solution. rhApoE2 proteins were used at a final concentration of 10 μg/mL. The fluorescence intensity was measured at 37 °C with an excitation of 440 nm and an emission of 484 nm for up to 10 days using Molecular Devices SpectraMax iD3 Multi-Mode Microplate Reader (Sunnyvale, CA).

2.13. Statistical analysis

Data are presented as mean ± standard deviation. For comparisons between two groups, Student's *t*-test was used; for comparisons involving multiple groups, one-way or two-way ANOVA with Turkey's or Dunnett's post-hoc test was used. All statistical analyses were conducted using Prism 6 software (GraphPad Software Inc., CA). The statistical significance is indicated by * $p < 0.05$, ** $p < 0.01$, *** $p < 0.001$, and **** $p < 0.0001$.

3. Results

3.1. ApoE protein in the human brain is highly sialylated, whereas minimal sialylation occurs in mouse brain ApoE

It is well-established that ApoE protein is expressed in a species, tissue, and cell-specific manner (Bu, 2009; Hatters et al., 2006; Hauser et al., 2011; Huang et al., 2004). Furthermore, LC-MS/MS studies have identified the sugar structures of ApoE glycoforms and cellular and secreted ApoE in brain tissue and CSF (Flowers et al., 2020; Halim et al., 2013; Lee et al., 2010). Human ApoE protein is a 299 aa protein that contains an N-terminal 18 aa signal sequence and a total of seven *O*-linked glycosylation sites: Thr8, Thr18, Thr194, Ser197, Thr289, Ser290, and Ser296. Among these identified sites, Thr289 (in humans) is the only residue conserved between human and mouse, although their sequence identity shows 71.6% (Fig. 1A). Moreover, our analyses indicated that the ApoE expression pattern was significantly different in

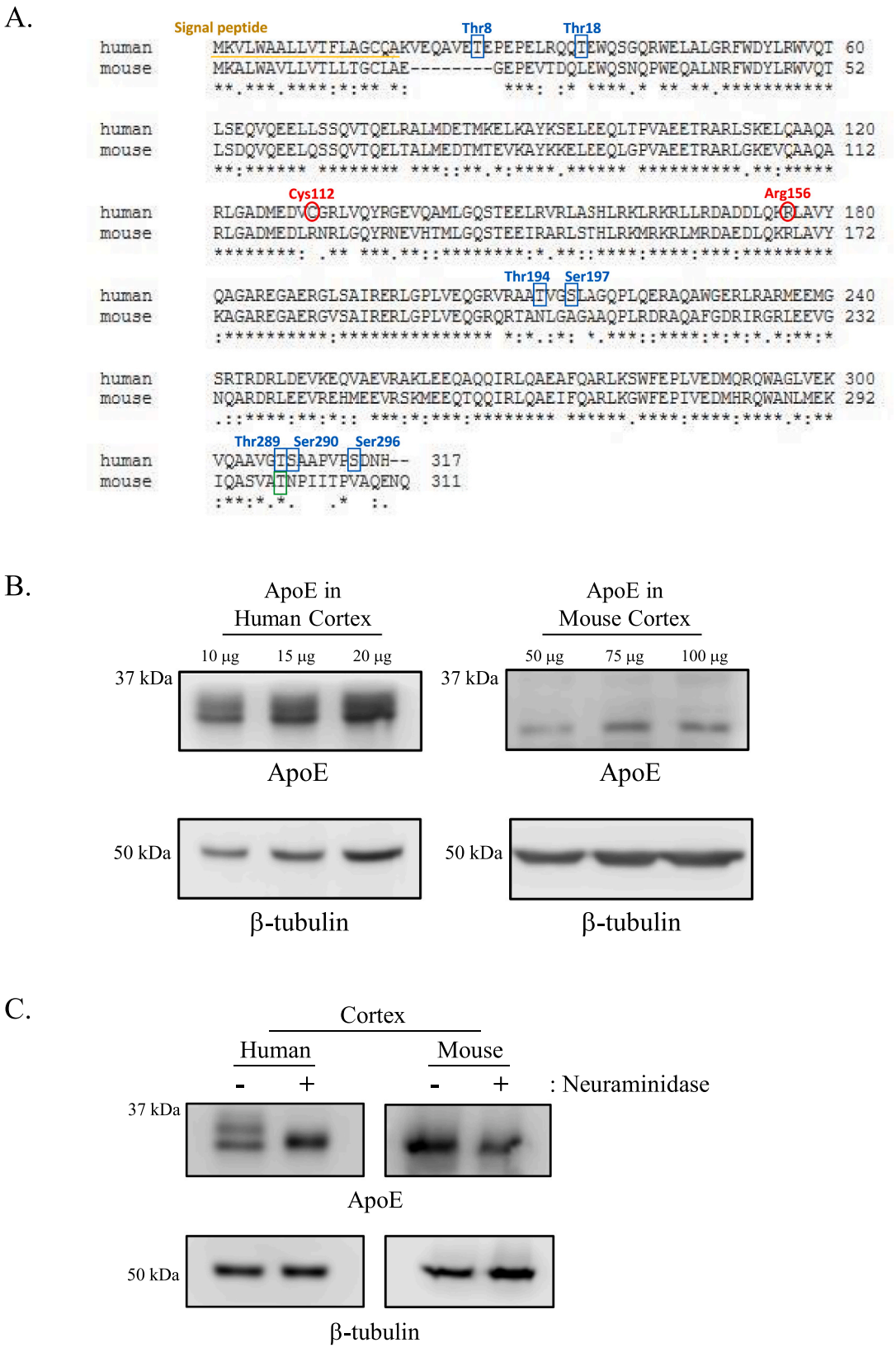

Fig. 1. Sialylation profiles of ApoE protein in the human brain in comparison with ApoE in the mouse brain. (A) Protein sequence alignment of human and mouse ApoE (human ApoE3 is shown). The three major isoforms of human ApoE differ by two amino acid residues at 112 and 158 (indicated by red circles): ApoE2 (Cyc112, Cys158), ApoE3 (Cys112, Arg158), and ApoE4 (Arg112, Arg158). Human ApoE contains seven *O*-linked glycosylation residues (indicated by blue squares), whereas there is only one residue (indicated by green square; corresponding to Thr289 in human ApoE) present in mouse ApoE. **(B)** Human and mouse brain cortex lysates were analyzed by SDS-PAGE and blots were probed for ApoE immunoreactivity with anti-ApoE antibodies. **(C)** Human and mouse brain cortex lysates were treated with neuraminidase or buffer alone; protein samples were then analyzed by SDS-PAGE and probed for ApoE immunoactivity using anti-ApoE antibodies. (For interpretation of the references to colour in this figure legend, the reader is referred to the web version of this article.)

human cortex lysates when compared to mouse cortex lysates. Multiple ApoE immunoreactive bands were detected in the human cortex with only one major band at a lower molecular weight observed in mouse cortex (Fig. 1B).

To verify that the observed higher MW bands are sialylated forms of ApoE protein, cortex lysates were treated with neuraminidase and analyzed by Western blot. Should the higher MW bands represent sialylated ApoE, then neuraminidase treatment prior to immunoblotting should result in the detection of only native ApoE (34 kDa_ApoE). As expected, treatment of human cortex lysates with neuraminidase resulted in the disappearance of the previously observed higher MW bands. By contrast, no change was observed in the ApoE immunoreactive band detected in mouse cortex lysates following treatment with neuraminidase (Fig. 1C). Collectively, these data indicate that ApoE protein in the human cortex is highly sialylated whereas ApoE protein in the mouse cortex is minimally sialylated or nonsialylated; data which is

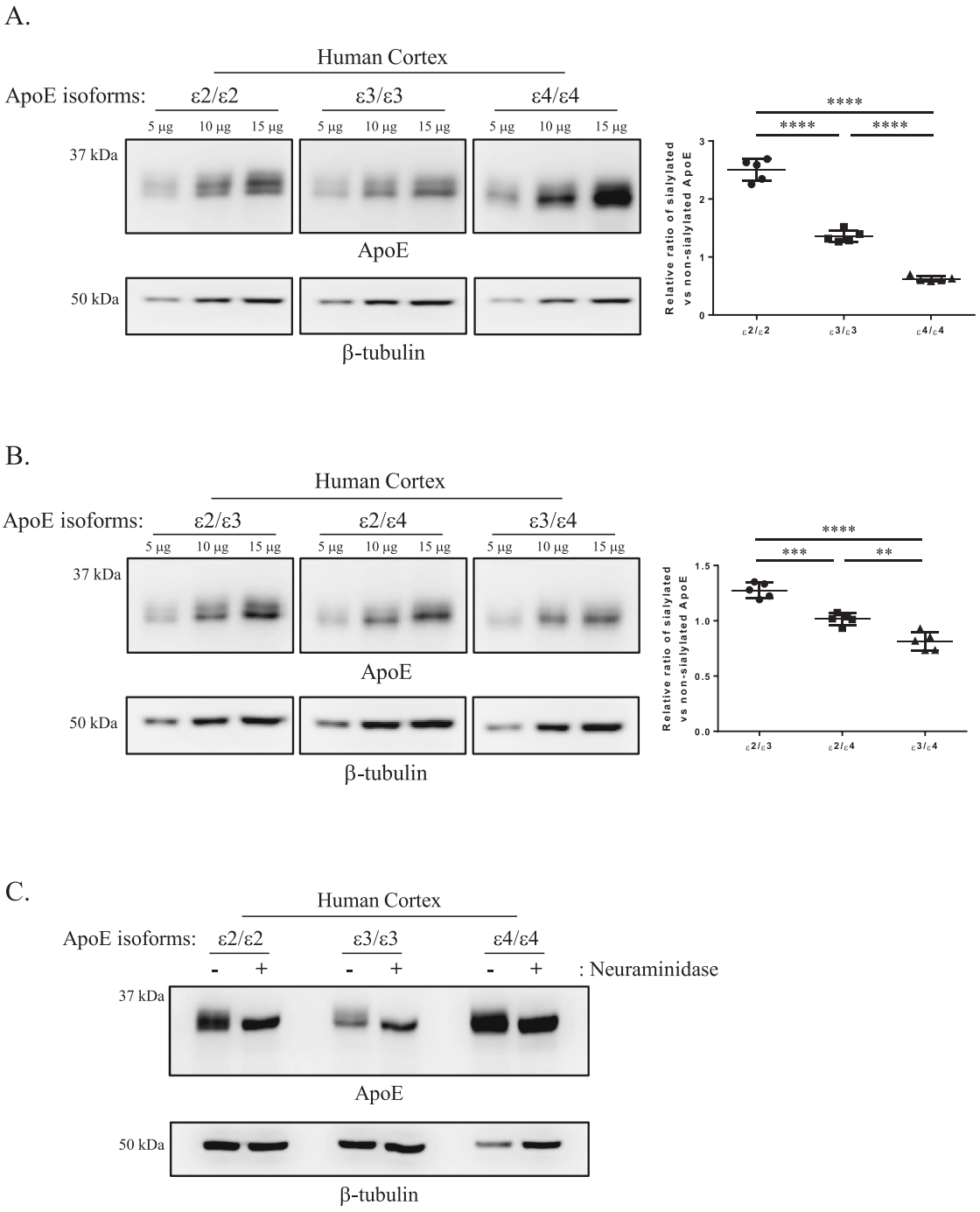

Fig. 2. Sialylation profiles of ApoE protein isoforms in human postmortem brain tissues. (A) Human postmortem brain cortical tissue lysates from homozygous carriers of *APOE* alleles (ε2/ε2, ε3/ε3, ε4/ε4) were analyzed by immunoblotting. Blots were probed for ApoE immunoreactivity and the intensity ratio of the upper_ApoE bands versus the lower_ApoE band for each genotype was quantitated. **(B)** Human postmortem brain cortical tissue lysates from heterozygous carriers of *APOE* alleles (ε2/ε3, ε2/ε4, ε3/ε4) were analyzed by immunoblotting. Blots were probed for ApoE immunoreactivity and the intensity ratio of the upper_ApoE bands versus the lower_ApoE band for each genotype was quantitated. Results are presented as mean ± standard deviation. $^{**}p < 0.01$, $^{***}p < 0.001$, and $^{****}p < 0.0001$. **(C)** Brain cortical tissue lysates from *APOE* homozygotes (ε2/ε2, ε3/ε3, ε4/ε4) were treated with neuraminidase and probed for ApoE immunoactivity, confirming the upper_ApoE bands represent sialylated_ApoE.

consistent with glycosylation residues' presence in respective protein sequences (Fig. 1A).

3.2. ApoE protein isoforms in the human brain are differentially sialylated

To determine whether the sialylation profile of human ApoE differs between isoforms (ApoE2, ApoE3, ApoE4), ApoE protein expression was first comparatively analyzed in human postmortem cortex samples identified as carriers of homozygous genotypes (ε2/ε2, ε3/ε3, ε4/ε4). Western blot data indicated distinct variations in the sialylation pattern of human ApoE isoproteins in the brain cortex. Two major forms of ApoE (lower_ApoE and upper_ApoE) were readily detected in carriers of *APOE* ε2/ε2 and ε3/ε3 genotypes. By contrast, the upper_ApoE band was significantly reduced in the brain cortex of ε4/ε4 carriers (Fig. 2A). Quantification indicated that the average intensity ratio between the upper_ApoE band and the lower_ApoE band was 2.50 for ε2/ε2, 1.36 for ε3/ε3, and 0.62 for the ε4/ε4 genotype (Fig. 2A). To confirm whether the upper_ApoE protein form represents sialylated ApoE, human cortex samples were treated with neuraminidase and analyzed by immunoblot. Consistent with previous data, treatment with neuraminidase resulted in the loss of the high MW ApoE immunoreactive band, regardless of ApoE genotype. No change was observed in the MW of the lower_ApoE immunoreactive band, confirming that the lower_ApoE protein form represents nonsiaylated_ApoE (native_ApoE; Fig. 2C).

Further analysis of the sialylation patterns in heterozygous *APOE* allele carriers (ε2/ε3, ε2/ε4, ε3/ε4) demonstrated that, as expected, ApoE protein in human cortex lysates carrying one copy of ε4 (i.e., ε2/ε4 or ε3/ε4) showed less sialylation than the samples from ε2/ε3 carriers, with an average intensity ratio between sialylated_ApoE and non-sialylated_ApoE of 1.45, 1.02, and 0.81 for the ε2/ε3, ε2/ε4, and ε3/ε4 genotype, respectively (Fig. 2B). Together, these data indicate that human ApoE protein isoforms are subjected to differential post-translational sialylation modifications, with ApoE2 being the most extensively sialylated and ApoE4 being the least sialylated. The degree of sialylation within the ApoE genotypes is as follows: ε2/ε2 > ε2/ε3 > ε3/ε3 > ε2/ε4 > ε3/ε4 > ε4/ε4.

3.3. The sialylated form of human ApoE is predominantly expressed as a secreted protein

Our initial discovery of the variations in sialylation of human ApoE protein isoforms in postmortem brain samples was further validated in the human neuroblastoma SH-SY5Y cell line. Cells were transfected with human ApoE isoform constructs (pCMV6-ApoE2, pCMV6-ApoE3, and pCMV6-ApoE4), and both cell lysates and culture media were collected and analyzed by immunoblot for ApoE expression. Consistent with the expression profiles observed in the human postmortem cortex (Fig. 2A), significantly more sialylated_ApoE was observed in SY5Y-ApoE2 than in the other two isotypes, with a minimum amount detected in SY5Y-ApoE4. Specifically, sialylated_ApoE was found predominantly in culture media as a secreted form (Fig. 3A, lower panel). By contrast, non-sialylated_ApoE appeared as the primary form in cell lysates with similar expression levels observed among the three isotypes (Fig. 3A). A pull-down assay was performed on culture media, which provided a secondary confirmation for the distinct sialylation pattern of the three ApoE isoproteins. Similar to the quantitative data generated from the postmortem cortex, the intensity ratio of the upper sialylated versus the lower nonsialylated form of ApoE protein in the culture media was 2.26 for SY5Y-ApoE2, 1.23 for SY5Y-ApoE3, and 0.78 for SY5Y-ApoE4 (Fig. 3A, lower panel).

To determine whether human ApoE transiently expressed in SH-SY5Y cells are comparable to the physiological form of human ApoE, both cell lysate and media fraction collected from the SY5Y-ApoE3 culture were treated with endoglycosidases and analyzed by immunoblot. The glycosylation of the ApoE3 protein was not affected by PNGase F and Endo H, confirming that human ApoE protein is not a target for *N*-linked glycosylation. By contrast, the loss of the upper ApoE immunoreactive band following treatment with a combination *O*-glycosidase and neuraminidase validates that human ApoE protein is exclusively targeted for *O*-linked glycan modification (Fig. 3B). Moreover, consistent with the human cortex data, the upper_ApoE was removed by digestion with neuraminidase for all ApoE isoforms (Fig. 3C).

3.4. Production and characterization of physiologically relevant and human-like recombinant ApoE2 (rhApoE2) glycoprotein

Previous literature indicates that human ApoE protein is highly glycosylated via *O*-linked glycans (Flowers et al., 2020; Halim et al., 2013; Lee et al., 2010). In the present study, we further demonstrate that human ApoE protein isoforms undergo differential sialylation, with ApoE2 most extensively sialylated. The next set of experiments was designed to evaluate the potential role of the sialic acid modification in the modulation of the biological properties of ApoE isoforms. We were particularly interested in addressing the question of whether the sialic acid residues present on the ApoE2 isoform could play a role in conferring ApoE2-mediated resistance against AD.

In order to adequately answer this question, pure and human-like ApoE2 protein was required. However, the commercially available recombinant human ApoE2 (rhApoE2) protein is primarily derived from *E. coli* which lacks the internal capabilities of facilitating human protein glycosylation; a fact confirmed by the detection of a single band at 34 kDa which corresponds to the expected size of native human ApoE (Fig. 4B). To establish an expression system which produces physiologically relevant and human-compatible recombinant ApoE2, a mammalian expression vector for ApoE2 with the C-terminus fused with a Strep-tag, pcDNA3.1(-)-hApoE2-Strep was established. FreeStyle 293-F cells, a suspension culture expression system, were then transfected with pcDNA3.1(-)-hApoE2-Strep to express recombinant human ApoE2. The culture medium was collected, concentrated, and purified using a gravity flow Strep-Tactin superflow column to obtain pure rhApoE2 (> 95% purity) with a yield of 30–35 mg protein/L culture (Fig. 4A). Nearly identical to the ApoE2 expressed in the human cortex, rhApoE2 derived from 293-F cells presents two major bands indicating posttranslational modification, which is deficient in rhApoE2 derived from *E. coli*. The intensity ratio of sialylated_ApoE2 versus nonsialyatled_ApoE2 in 293-F cells-derived rhApoE2 was not significantly different from ApoE2 in human brain tissue, further demonstrating the compatibility of 293-F-rhApoE2 with the human form of ApoE2 (Fig. 4B).

Moreover, treatment with deglycosylation enzymes that specifically target *N*-linked glycans (PNGase F and Endo H) did not alter the ApoE immunoreactive bands, indicating the lack of *N*-linked glycans in 293-F-rhApoE2. As expected, treatment with neuraminidase alone or in combination with *O*-glycosidase resulted in the disappearance of the upper band, indicating that 293-F-rhApoE2 is a sialic acid-enriched protein (Fig. 4C). Collectively, these data confirm that rhApoE2 derived from 293-F cells is posttranslationally modified by *O*-linked glycosylation and sialylation; these structural profiles are consistent with physiological patterns of ApoE2 protein expressed in the human brain.

3.5. The sialic acid moiety in human ApoE2 attenuates ApoE2-Aβ binding and Aβ fibrillation

Many studies have reported the formation of complexes between ApoE and Aβ *in vitro* and *in vivo* (Aleshkov et al., 1997; Bentley et al., 2002; LaDu et al., 1994; Verghese et al., 2013; Zhou et al., 1996). However, the ApoE protein isoform-specific difference in ApoE-Aβ interaction and the effect of the complex remains controversial. To examine the impact of the ApoE sialylation on the formation of SDS-stable ApoE-Aβ complexes, a binding study using rhApoE2 derived from *E. coli* and 293-F cells was performed and analyzed. A more significant rhApoE2-Aβ interaction and complex formation with both Aβ40

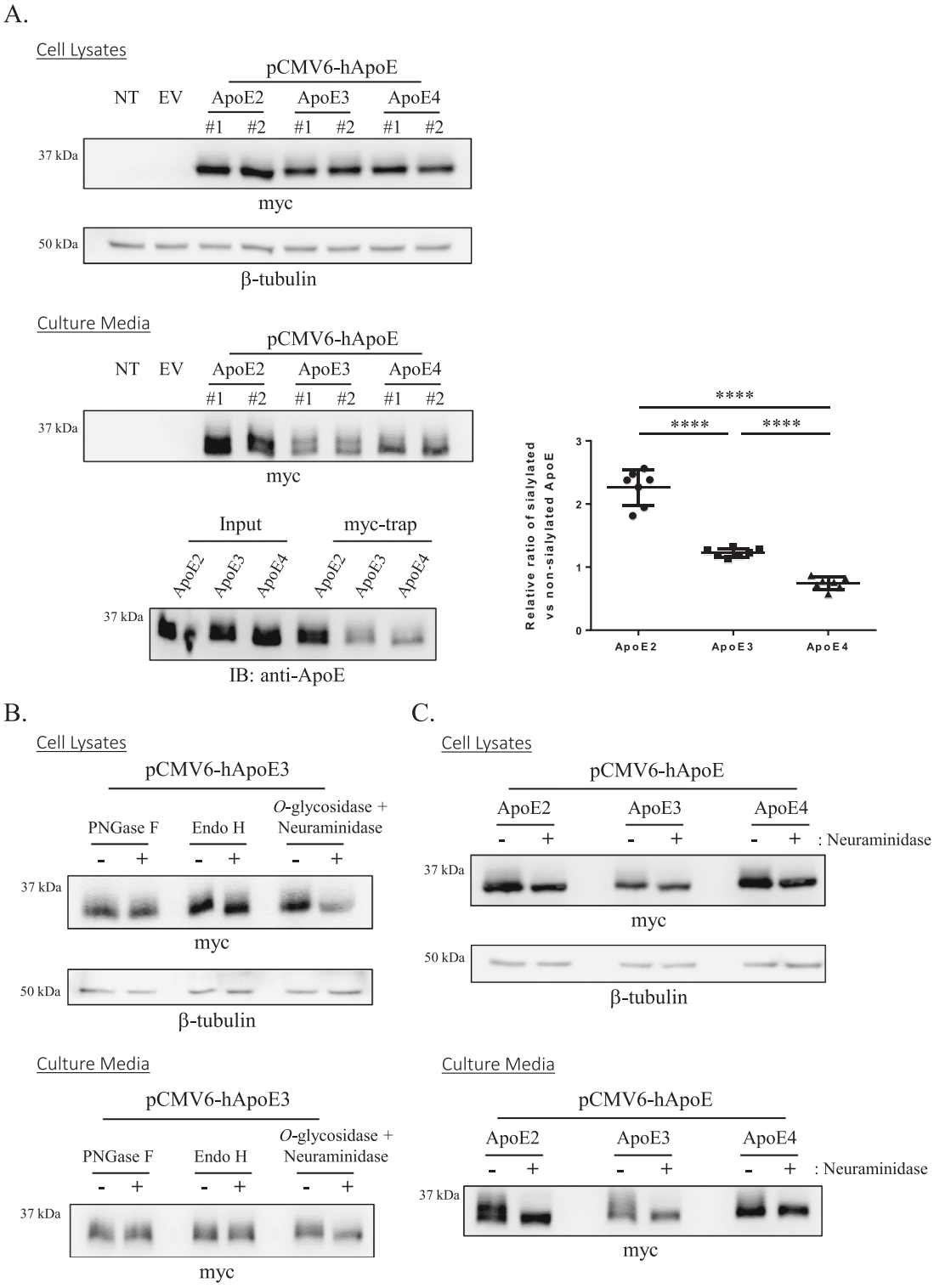

Fig. 3. Sialylation profiles of human ApoE protein isoforms expressed in SH-SY5Y cells. (A) Empty vector (pCMV6-Entry), myc-tagged pCMV6-human ApoE2, pCMV6-human ApoE3, or pCMV6-human ApoE4 constructs were transfected into human SH-SY5Y cells. Cell lysates and culture media fractions were harvested and probed for ApoE immunoreactivity using anti-myc antibodies. Pull-down assay was performed with myc-trap on culture media fractions. Results are shown as the intensity ratio of sialylated_ApoE versus nonsialylated_ApoE and presented as mean ± standard deviation. ****$p < 0.0001$. **(B)** Myc-tagged pCMV6-human ApoE3 construct was transfected into SH-SY5Y cells. Cell lysates and culture media were harvested and treated with endoglycosidases (PNGase F, Endo H, *O*-glycosidase, and neuraminidase). The resulting samples were analyzed for ApoE immunoreactivity using anti-myc antibodies. **(C)** Myc-tagged pCMV6-human ApoE2/ApoE3/ApoE4 constructs were transfected into SH-SY5Y cells. Cell lysates and culture media were harvested, treated with neuraminidase, and probed for ApoE immunoreactivity using anti-myc antibodies.

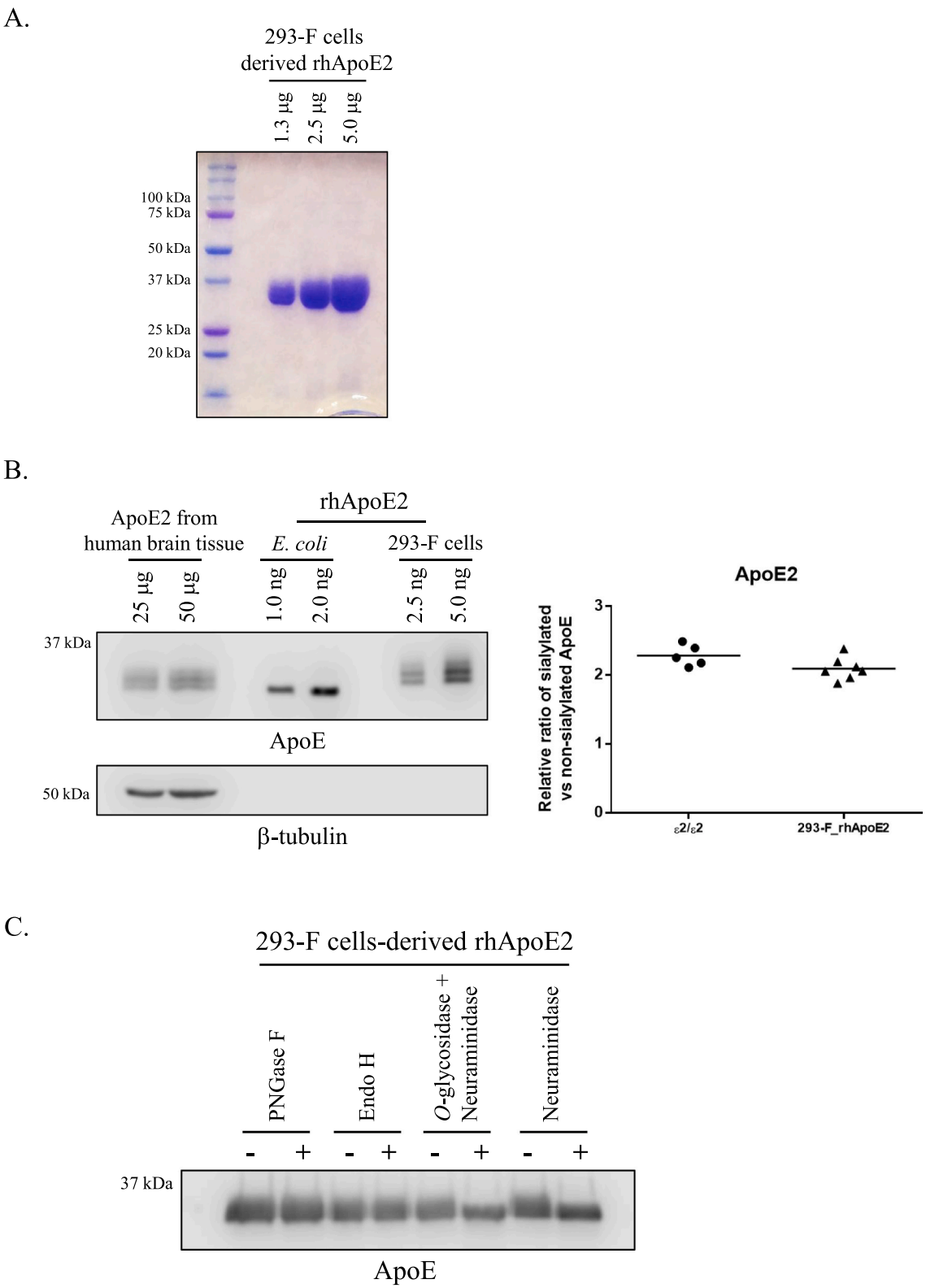

Fig. 4. Production and characterization of physiologically relevant and human-like rhApoE2 glycoprotein. (A) The purity of recombinant human ApoE2 derived from 293-F cells was analyzed by SDS-PAGE. **(B)** Sialylation profiles of ApoE2 protein derived from human brain tissue lysates, *E. coli*, or 293-F cells were comparatively analyzed by immunoblotting. Results are shown as the intensity ratio of sialylated_ApoE2 versus nonsialylated_ApoE2 expressed in human brain tissues of ApoE ε2/ε2 homozygotes in comparison with ApoE2 derived from 293-F cells and presented as mean ± standard deviation. **(C)** Deglycosylation analyses were performed on rhApoE2 derived from 293-F cells using specific endoglycosidase: PNGase F, Endo H, *O*-glycosidase, and neuraminidase. The resulting samples were analyzed by immunoblotting using anti-ApoE antibodies.

and Aβ42 peptides, as indicated by a greater band intensity, was observed with rhApoE2 derived from *E. coli* (non-sialyalted_rhApoE2) when compared with rhApoE2 derived from 293-F cells (sialyalted_rhApoE2). These results indicate that the sialylated structure on the ApoE2 protein negatively affects ApoE2 binding affinity for Aβ and consequently reduces ApoE2-Aβ complex formation (Fig. 5A and B). It should be noted that the polyclonal antibody used to detect ApoE was not equally reactive within all reactions, especially in the presence of the Aβ42 peptide. This may be due to the ApoE antibody epitope on ApoE being partially masked in the complex structure of ApoE-Aβ42. An immunoprecipitation was then performed on complexes of sialylated_rhApoE2 versus desialylated_rhApoE2 with Aβ40. rhApoE2 derived from 293-F cells was treated with neuraminidase. Desialylated_rhApoE2 was confirmed by WB (Fig. 5C). ApoE was detected only in the desialylated_rhApoE2-Aβ40 preparation (Fig. 5D), providing further evidence that the sialic acid moiety in ApoE modulates ApoE-Aβ interaction and the removal of sialic acid increases the binding affinity of ApoE for Aβ peptides.

To further investigate the effect of the sialic acid component of ApoE on the formation of the ApoE-Aβ complex, the binding affinities of sialylated_rhApoE2 versus desialylated_rhApoE2 with three different regions of Aβ peptide (Aβ1–16, Aβ12–28, and Aβ25–35) were comparatively analyzed. We observed no difference between sialylated_rhApoE2 and desialylated_rhApoE2 in their binding with Aβ1–16 (Fig. 5E) and Aβ25–35 (Fig. 5G); however, desialylated_rhApoE2 exhibited a significantly greater affinity for the Aβ12–28 fragment than sialylated_rhApoE2 (Fig. 5F). These data indicate that the sialic acid structure in ApoE attenuates ApoE interaction specifically with the midregion of Aβ peptides (residues 17–24; Fig. 5H).

A thioflavin T (ThT) aggregation assay was next performed to evaluate the impact of ApoE sialylation on Aβ42 fibril formation. In the assay, an increase in the fluorescence signal indicates an increase in Aβ42 fibril formation. The results showed that Aβ42 fibrillation was significantly increased by the coincubation of Aβ42 with desialyalted_rhApoE2 compared with sialyalted_rhApoE2 (Fig. 5I). These data, together with the binding results, indicate that the sialic acid modification in human ApoE protein attenuates ApoE binding affinity for Aβ and consequently reduces Aβ fibrillation (Fig. 5J).

4. Discussion

ApoE is well characterized as a glycosylated protein, exclusively *O*-linked, through serine or threonine residues (Flowers et al., 2020; Halim et al., 2013; Lee et al., 2010). Sialic acid typically occupies a terminal position on glycans, and it is a negatively charged carbohydrate implicated in the mediation of interactions with various receptors, ligands, and cofactors (Hayakawa and Varki, 2012; Yoo et al., 2015). Though ApoE in human brain tissue and CSF is heavily glycosylated, murine brain ApoE is minimally glycosylated. This is consistent with the sequence differences between human and murine ApoE which shown 7 glycosylation sites identified in human ApoE with only one conserved residue found in murine ApoE (Fig. 1A). Moreover, ApoE derived from the human CSF is shown to be more extensively glycosylated than ApoE from the plasma. The CSF ApoE has sialic acid residues that are 10-fold more abundant in the C-terminal lipid-binding domain (Thr289, Ser290, and Ser296) than plasma ApoE. In contrast, plasma ApoE holds greater sialylation in the N-terminal receptor-binding domain (Thr8). The hinge domain (Thr194 and Ser197) undergoes similar glycosylation for both plasma and CSF-derived ApoE (Chernick et al., 2019; Flowers et al., 2020). To date, the exact role of the sialic acid moiety expressed on human ApoE protein in its physiological function is unknown.

Human ApoE, the most prevalent genetic risk factor for LOAD, exists as three isoforms (ApoE2, ApoE3, and ApoE4), with ApoE4 conferring significant LOAD risk and ApoE2 providing neuroprotection (Farrer et al., 1997; Kim et al., 2009; Liu et al., 2013; Wu et al., 2018). The three isoforms differ by just two amino acids in the protein, but their impact on AD outcomes is immense. In the present study, we demonstrate, for the first time, the distinct differences in sialylation patterns among human ApoE protein variants in human brain tissues and human brain-derived cell lines. ApoE2 exhibits more sialic acid modification than ApoE3, and ApoE4 displays the least sialylation among the three isoforms. These data suggest that differential profiles of sialylation in ApoE protein may cause distinctive effects in AD pathologies. Several studies have demonstrated that ApoE4 and ApoE2 isoforms are associated with a more closed or open conformation, respectively, than ApoE3 (Dong et al., 1996; Dong and Weisgraber, 1996; Kara et al., 2017; Mahley et al., 2009). Arg112 in ApoE4 causes the Arg61 side-chain to extend away from the helix bundle, interacting with Glu255 and resulting in a compact closed structure (Zhong and Weisgraber, 2009). We hypothesize that the structural differences might affect sialylation patterns in ApoE isoforms; however, more areas for research remain to be identified.

The biosynthesis of sialic acid starts with uridine 5′-diphosphate-*N*-acetyl-D-glucosamine (UDP-GlcNAc). UPD-GlcNAc is a nucleotide sugar and is synthesized through the hexosamine biosynthetic pathway (HBP). In the HBP, the glucosamine-6-phosphate is synthesized from fructose-6-phosphate, an intermediate metabolite derived from glucose (Galeano et al., 2007; Keppler et al., 1999; Xu et al., 2017). Thus, in essence, sialic acid production is directly controlled by glucose metabolism, precisely, the initial two steps that lead to the generation of fructose-6-phosphate, in which hexokinase (HK) plays a critical role. Previously, we demonstrated that ApoE2 brains have the most robust glycolytic profile due to increased HK expression (Wu et al., 2018). Therefore, it can be speculated that the production of sialic acid is significantly affected by the status of HK. Several studies have demonstrated that glucose utilization in the brain is affected by the *APOE* genotype, and the ApoE4 individuals were shown to have lower glucose uptake on an FDG PET scan (Brandon et al., 2018; Perkins et al., 2016; Reiman et al., 2004). Together, these findings suggest that a greater degree of sialylation in ApoE2 protein could be a consequence of high glucose metabolism in the brain. However, this hypothesis, along with the potential role of other metabolic events involved in protein glycosylation and sialylation, needs to be experimentally examined.

Numerous *in vitro* and *in vivo* studies indicate an isoform-specific role of ApoE in the metabolism of Aβ peptides in the brain (Aleshkov et al., 1997; Bentley et al., 2002; LaDu et al., 1994; Manelli et al., 2004; Strittmatter et al., 1993). The isoform-specific ApoE-Aβ interaction may contribute to the effects of isoform specificity in AD development. Several studies have shown that ApoE facilitates Aβ clearance and thus reduces Aβ aggregation; conversely, some studies have reported the role of ApoE as enhancing the fibrillization of Aβ (Nielsen et al., 2010; Tai et al., 2014). These contradictory results arise likely due to the heterogeneous nature of both ApoE and Aβ. Thus, understanding ApoE-Aβ interaction is critically important for elucidating the isoform-specific role of ApoE in AD. However, the key contributor in ApoE-Aβ binding remains largely unclear. Sialic acid is well demonstrated for its role in the mediation of molecular recognition and interaction, suggesting that the sialylation modification of ApoE might serve crucial functions in the human brain. We, therefore, evaluated whether the sialic acid residues in ApoE protein affected ApoE-Aβ interaction; consequently, these data would provide meaningful indications regarding the biological importance of sialylation of ApoE in the CNS. We found that both sialylated (derived from 293-F cells) and nonsialylated rhApoE2 (derived from *E. coli*) bound with Aβ40 and Aβ42 *in vitro*. However, the binding of Aβ with nonsialylated rhApoE2 was significantly greater than with sialylated rhApoE2, indicating that the sialylation status in these two different forms of rhApoE2 played a role in their binding with Aβ peptides. In support of our observations, it was found that in a human APP transgenic mouse model, expression of murine ApoE accelerated Aβ fibril formation. In comparison, expression of human ApoE, in particular the ApoE2 isoform (and ApoE3 to a lesser extent), markedly delayed Aβ deposition (Fagan et al., 2002). It can be speculated that the differential

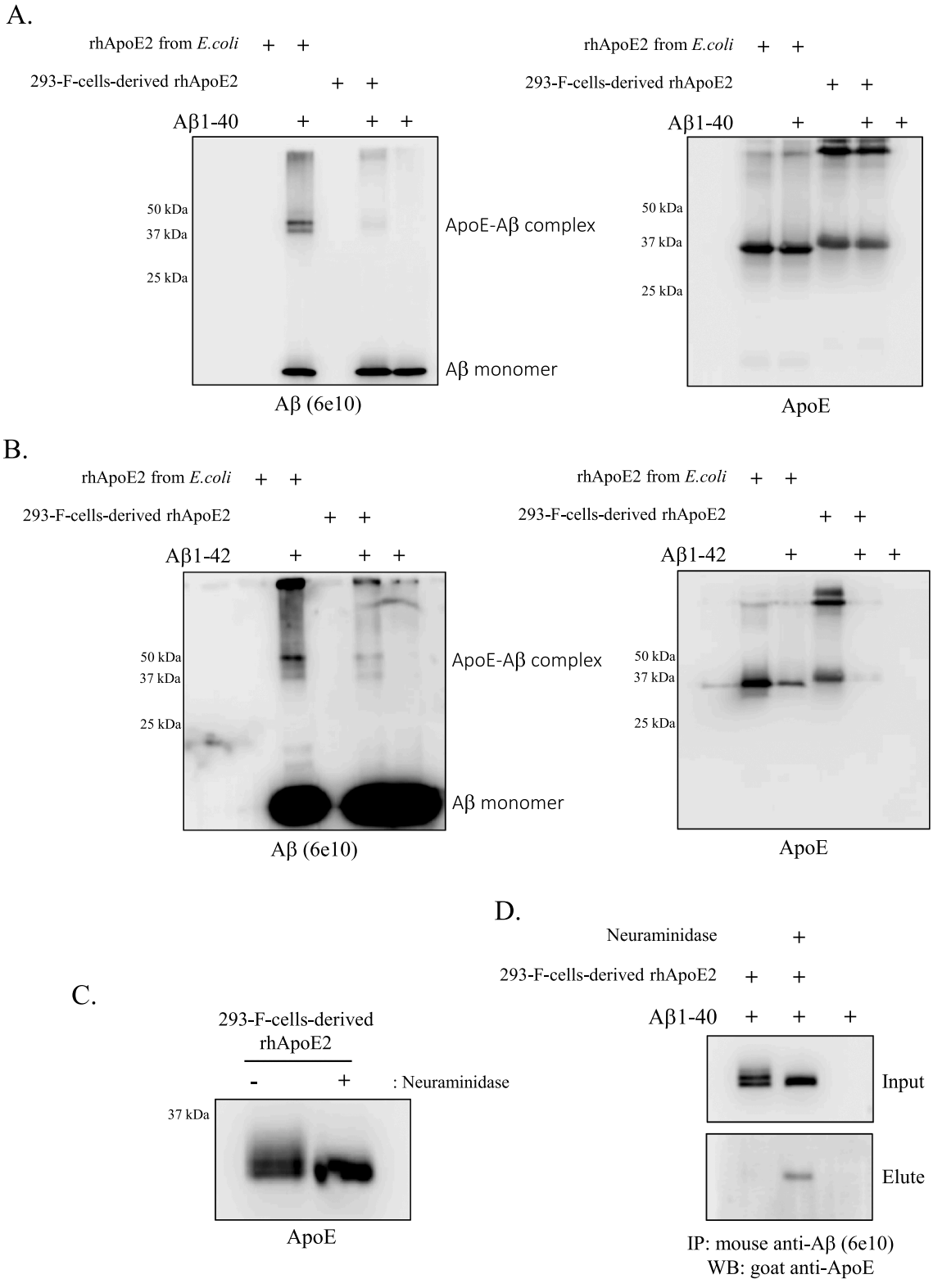

Fig. 5. The sialic acid moiety in human ApoE affects ApoE-Aβ binding and Aβ fibrillation. (A-B) Following a 2 h at 37 °C incubation of rhApoE2 derived from *E. coli* or 293-F cells with Aβ peptides, the rhApoE2-Aβ40 (A) and rhApoE2-Aβ42 (B) complexes were analyzed by SDS-PAGE and probed for Aβ and ApoE immunoreactivities. **(C)** Sialyalted_rhApoE2 (derived from 293-F cells) vs desialylated_rhApoE2 (prepared from rhApoE2 derived from 293-F cells and treated with neuraminidase) were confirmed by immunoblotting. **(D)** Sialylated_rhApoE2-Aβ40 and desialylated_rhApoE2-Aβ40 complexes were immunoprecipitated using anti-human monoclonal Aβ antibody (6e10). The elutes were probed for ApoE immunoreactivity using goat polyclonal ApoE antibody. **(E-G)** The interactions of sialylated_rhApoE2 versus desialyated_rhApoE2 with Aβ fragments: (E) Aβ1–16, (F) Aβ12–28, and (G) Aβ25–35, were analyzed by SDS-PAGE and probed for Aβ and ApoE immunoreactivities using specific antibodies as indicated. Quantitative results are shown as relative band intensity and presented as mean ± standard deviation. Each close circle and square in each graph is representative of one independent experiment ($n = 9$ for Aβ1–16, $n = 7$ for Aβ12–28, and $n = 6$ for Aβ25–35). $^{**}p < 0.01$. **(H)** The residues indicated in red represent the sequence region in Aβ that preferentially binds desialyated_rhApoE2. **(I)** Thioflavin T Aβ42 aggregation assay

was performed to analyze Aβ42 fibril formation influenced by sialylated_rhApoE2 in comparison with desialylated_rhApoE2. The graph is generated from one experiment but is representative of $n = 4$ independent repeats of the same assay. * $p < 0.05$, ** $p < 0.01$, and *** $p < 0.001$. **(J)** Data presented in this figure indicate that the sialic acid modification in human ApoE protein may serve as a key modulator of Aβ fibrillization. The removal of sialic acid increases ApoE binding affinity for Aβ17–24 residues and such an interaction may promote Aβ fibrillation. The presence of sialic acid attenuates ApoE binding with Aβ17–24 and reduces Aβ fibrillation. (For interpretation of the references to colour in this figure legend, the reader is referred to the web version of this article.)

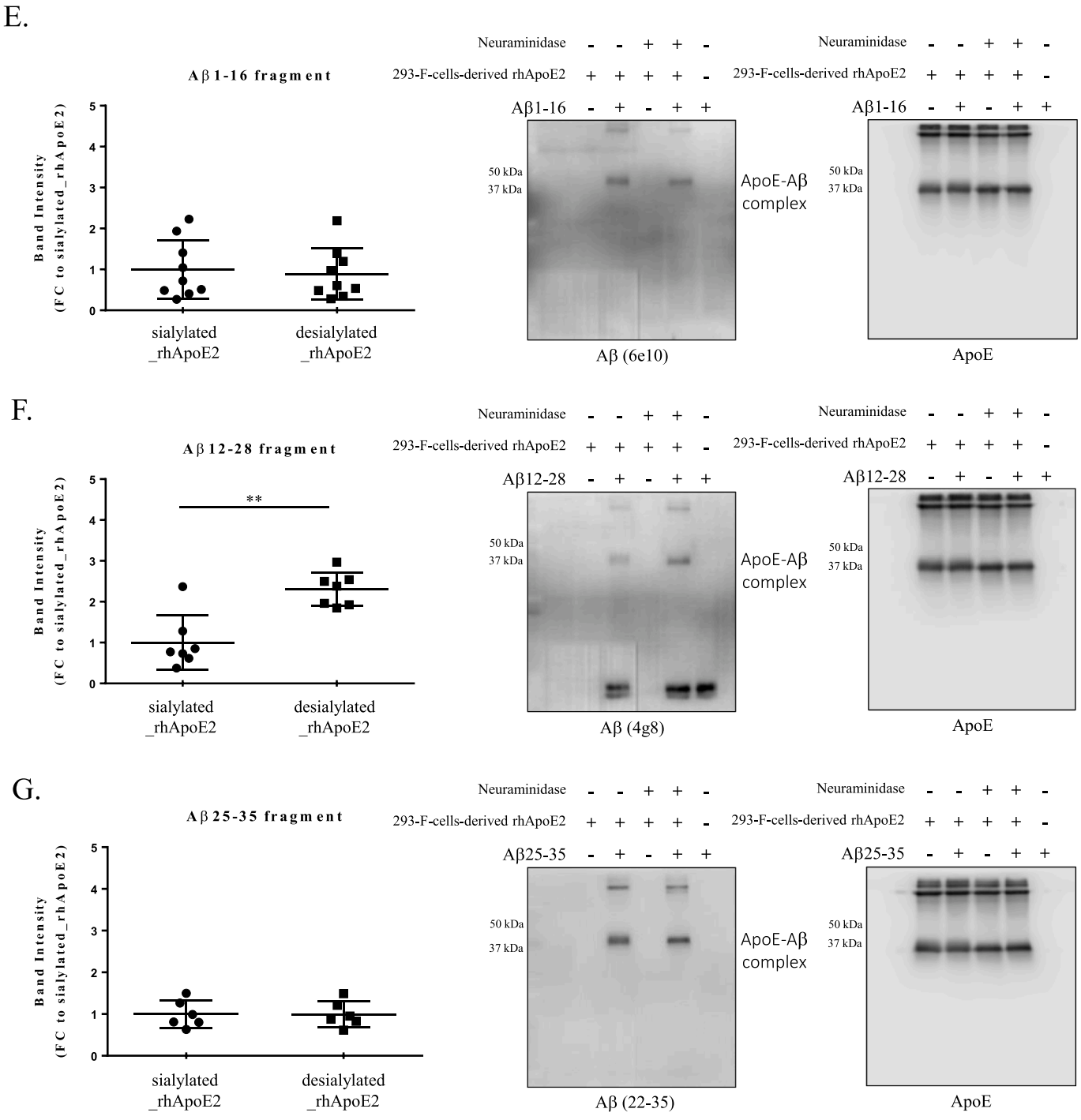

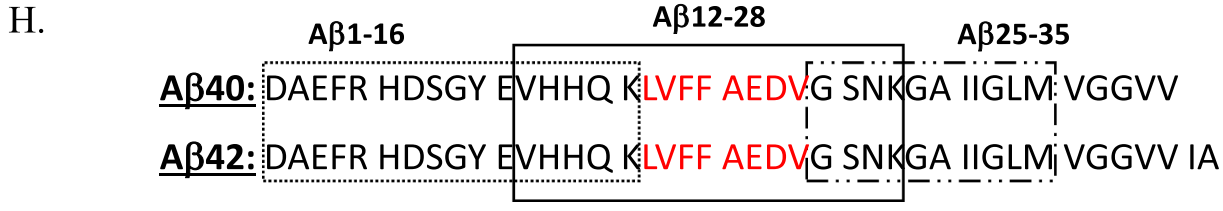

Fig. 5. (*continued*).

I.

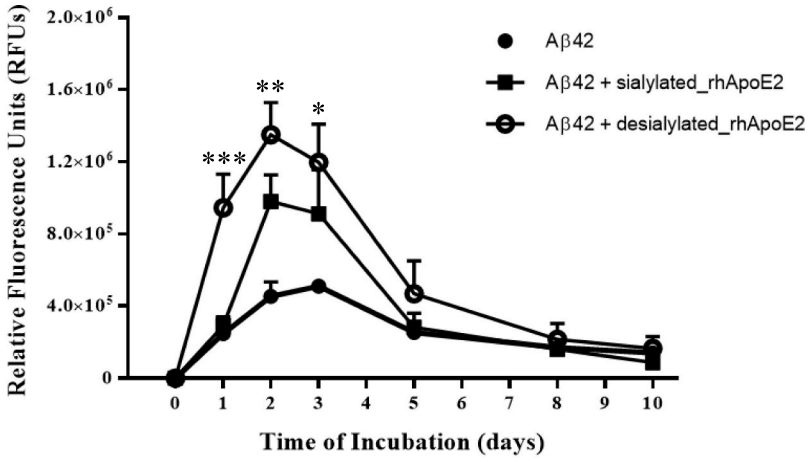

J.

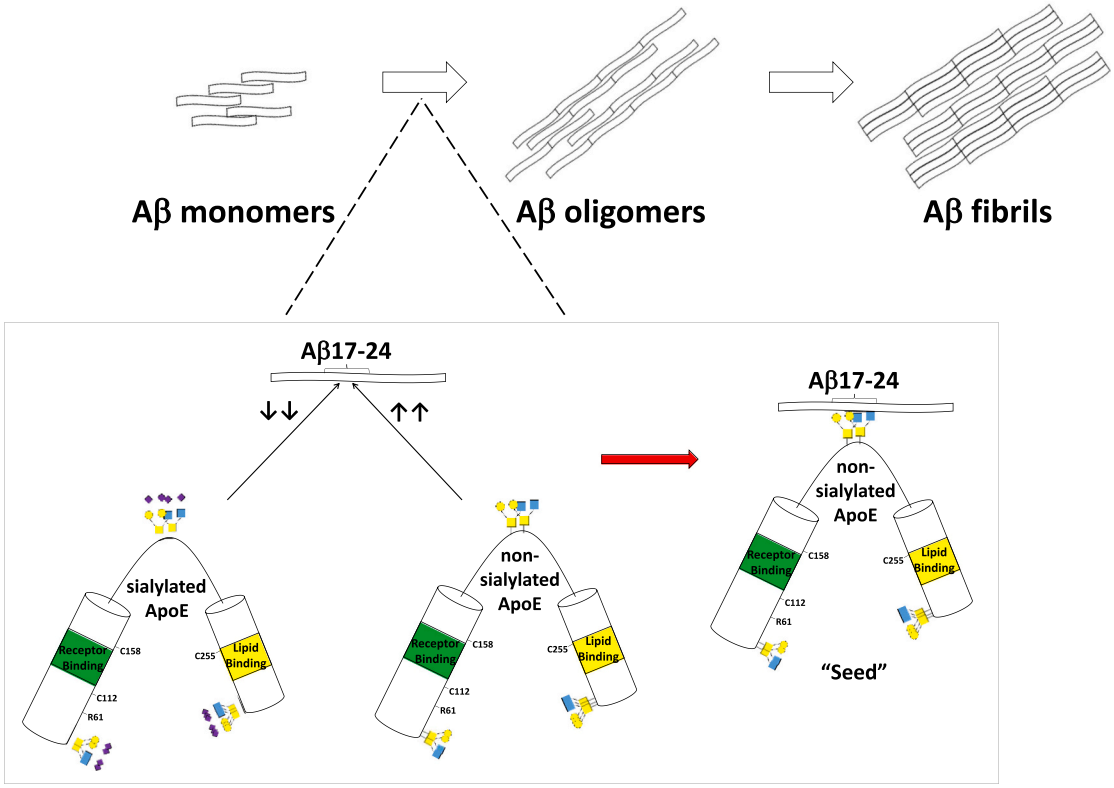

Fig. 5. (*continued*).

impact on Aβ metabolism by murine versus human ApoE may also be closely associated with the differences in their sialylation profiles. Together, these findings indicate that the presence of the sialic acid structure in ApoE reduces the binding affinity of ApoE for Aβ and thus formation of ApoE-Aβ complexes.

Disruption of the ApoE-Aβ interaction has been recently attempted as one of the therapeutic strategies for AD. This strategy has been tested in AD mouse models with monoclonal ApoE antibodies and small peptides (Kuszczyk et al., 2013; Pankiewicz et al., 2014; Sadowski et al., 2004). ApoE has a binding affinity to Aβ, and the ApoE-Aβ binding site was found primarily at 12–28 residues of Aβ (Strittmatter et al., 1993). Thus, Aβ12–28P, a small peptide corresponding to the ApoE-binding motif within Aβ that competes with ApoE-Aβ binding at this region, was designed (Sadowski et al., 2004). Experiments with a neuronal-astrocytic culture system showed that Aβ12–28P reduced intraneuronal Aβ accumulation and synaptic degeneration (Kuszczyk et al., 2013). Experiments further demonstrated that Aβ12–28P reduced both soluble and insoluble Aβ levels and the Aβ plaque burden in two AD transgenic mouse models (Pankiewicz et al., 2014). The most recent study further showed that CPO_Aβ17–21P, a cyclic peptoid derived from Aβ12–28 that shows better bioavailability/biostability than Aβ12–28P, nearly completely blocked the binding of ApoE4-Aβ at an 8:1 molar ratio (peptoid:ApoE4) (Liu et al., 2017). Most interestingly, in this study, we observed that the terminal sialic acid moieties significantly

diminished the binding of ApoE to the Aβ12–28 fragment. When sialic acid was removed from ApoE with neuraminidase, the desialylated ApoE binding to Aβ12–28 fragment was more considerably impacted than other Aβ fragments (Aβ1–16 and Aβ25–35). These findings suggest that sialic acid in ApoE might modulate the ApoE-Aβ binding through Aβ17–24 residues (Fig. 5H), providing a reasonable explanation for the inhibition effect of ApoE-Aβ binding using the CPO_Aβ17–21P peptoid. Moreover, we found that the desialylated_ApoE accelerated the fibrillization of Aβ42 in the early stage (Fig. 5J), suggesting that the ApoE-Aβ binding through Aβ17–24 residues might serve as a "seed" for promoting Aβ aggregation. Overall, our findings shed important light on understanding how the three ApoE isoforms behave differently in the human brain, especially concerning their distinct roles in Aβ metabolism. Based on these findings, it would be plausible that the relatively low level of sialylation in ApoE4 would be a major contributor to the well-documented more potent interaction between ApoE4 and Aβ, a mechanism thought to underlie the ApoE4-mediated increased risk of Aβ pathogenesis associated with AD.

In light of the many prominent roles of sialic acid, particularly in the modulation of molecular recognition and cellular signaling (Rawal and Zhao, 2021), it can be reasonably speculated that the differential expression of sialic acid in ApoE isoproteins might also contribute to some of their other biological properties. In addition to Aβ binding, ApoE isoforms exhibit significantly divergent specificities in their interactions with lipids and lipoproteins. ApoE4 is shown to bind preferentially to VLDL, whereas ApoE2 and ApoE3 bind preferentially to HDL (Liu et al., 2013; Matsubara, 2012). In addition, ApoE4 is found to be poorly lipidated when compared with ApoE2 and ApoE3 (Hanson et al., 2013; Heinsinger et al., 2016; Hu et al., 2015). It is yet to be determined whether the sialic acid moiety in ApoE might be engaged in these interactions. Another area of importance involves the effect of ApoE isoforms on brain responses to inflammatory stimuli. With recent revelations that multiple AD risk genes are exclusively expressed by microglia, neuroinflammation has increasingly been recognized for its potentially critical roles in AD pathogenesis (Efthymiou and Goate, 2017; Hemonnot et al., 2019; Sierksma et al., 2020; Wightman et al., 2020). Siglecs, a family of sialic acid-binding immunoglobulin-type lectins that are predominantly expressed on the cell surfaces of microglia in the brain, serve as a pivotal anti-inflammatory mediator through which inhibitory signals are transmitted from sialic acid, resulting in microglial inactivation (Linnartz-Gerlach et al., 2014; Rawal and Zhao, 2021; Wightman et al., 2020). ApoE4 has been associated with a diminished capacity to suppress inflammatory stimuli *in vivo* and *in vitro* (Dorey et al., 2014; Guo et al., 2004). Further research is necessary to explore whether the sialic acid structure in ApoE might play a role in the modulation of Siglec activity and subsequent microglial inflammation. Moreover, recent studies have shown that in the CNS, in addition to astrocytes, ApoE is also de novo synthesized by microglia and neurons, although to a lesser extent (Aoki et al., 2003; Kara et al., 2017; Kockx et al., 2018; Xu et al., 2006). Specifically, neuronal ApoE constitutes about 20% of total brain ApoE, and the neuronal expression of ApoE is increased in response to injury (Aoki et al., 2003; Harris et al., 2004; Xu et al., 2006). Research has also indicated that different forms of ApoE from different cellular sources may exhibit quite different activities (Buttini et al., 2010; Huang, 2006; Huang et al., 2004; Van Dooren et al., 2006); however, the origin of these functional distinctions remains elusive. Future studies of cell-specific sialylation profiles of ApoE protein isoforms under both normal and neurodegenerative conditions will enable a better understanding of the influence of ApoE sialylation on brain health and diseases such as AD.

5. Conclusions

In the present study, we have shown that the three protein isoforms of human ApoE (ApoE2, ApoE3, and ApoE4) undergo varying degrees of sialylation, with ApoE2 exhibiting the most abundant while ApoE4 is the least sialylated. We have further shown that the sialic acid moiety in ApoE significantly affects ApoE-Aβ interaction and Aβ fibrillation. Specifically, the sialylation in ApoE2 reduces ApoE2 binding affinity for Aβ in the Aβ17–24 region and attenuates Aβ fibrillation. These findings implicate that the discrepancy in sialylation of ApoE protein isoforms may contribute to their distinct roles in AD pathogenesis, and it may be possible to modulate ApoE sialylation as an approach to AD prevention or even therapy.

Funding

This work was supported by grants from the National Institutes of Health (R01AG061038, R21AG059177) and the University of Kansas J. R. and Inez Jay Fund.

Author contribution statement

H.M. and L.Z. designed the experiments, analyzed the data, and wrote the manuscript. V.H. assisted with the studies involving human brain tissues. All authors read and approved the final version of the manuscript.

Declaration of Competing Interest

None.

Acknowledgments

We would like to thank the NIH NeuroBioBank for providing human brain tissue samples and Dr. Mure (University of Kansas, Lawrence, KS, USA) for providing the pEXPR-IBA42 vector.

References

Aleshkov, S., et al., 1997. Interaction of nascent ApoE2, ApoE3, and ApoE4 isoforms expressed in mammalian cells with amyloid peptide beta (1-40). Relevance to Alzheimer's disease. Biochemistry. 36, 10571–10580.
Aoki, K., et al., 2003. Increased expression of neuronal apolipoprotein E in human brain with cerebral infarction. Stroke. 34, 875–880.
Bentley, N.M., et al., 2002. Apolipoprotein E structural requirements for the formation of SDS-stable complexes with beta-amyloid-(1-40): the role of salt bridges. Biochem. J. 366, 273–279.
Brandon, J.A., et al., 2018. APOE and Alzheimer's disease: neuroimaging of metabolic and cerebrovascular dysfunction. Front. Aging Neurosci. 10, 180.
Bu, G., 2009. Apolipoprotein E and its receptors in Alzheimer's disease: pathways, pathogenesis and therapy. Nat. Rev. Neurosci. 10, 333–344.
Buttini, M., et al., 2010. Cellular source of apolipoprotein E4 determines neuronal susceptibility to excitotoxic injury in transgenic mice. Am. J. Pathol. 177, 563–569.
Chernick, D., et al., 2019. Peripheral versus central nervous system APOE in Alzheimer's disease: interplay across the blood-brain barrier. Neurosci. Lett. 708, 134306.
Dong, L.M., Weisgraber, K.H., 1996. Human apolipoprotein E4 domain interaction. Arginine 61 and glutamic acid 255 interact to direct the preference for very low density lipoproteins. J. Biol. Chem. 271, 19053–19057.
Dong, L.M., et al., 1996. Novel mechanism for defective receptor binding of apolipoprotein E2 in type III hyperlipoproteinemia. Nat. Struct. Biol. 3, 718–722.
Dorey, E., et al., 2014. Apolipoprotein E, amyloid-beta, and neuroinflammation in Alzheimer's disease. Neurosci. Bull. 30, 317–330.
Efthymiou, A.G., Goate, A.M., 2017. Late onset Alzheimer's disease genetics implicates microglial pathways in disease risk. Mol. Neurodegener. 12, 43.
Fagan, A.M., et al., 2002. Human and murine ApoE markedly alters a beta metabolism before and after plaque formation in a mouse model of Alzheimer's disease. Neurobiol. Dis. 9, 305–318.
Farrer, L.A., et al., 1997. Effects of age, sex, and ethnicity on the association between apolipoprotein E genotype and Alzheimer disease. A meta-analysis. APOE and Alzheimer disease Meta analysis consortium. Jama. 278, 1349–1356.
Flowers, S.A., et al., 2020. O-glycosylation on cerebrospinal fluid and plasma apolipoprotein E differs in the lipid-binding domain. Glycobiology. 30, 74–85.
Galeano, B., et al., 2007. Mutation in the key enzyme of sialic acid biosynthesis causes severe glomerular proteinuria and is rescued by N-acetylmannosamine. J. Clin. Invest. 117, 1585–1594.

Guo, L., et al., 2004. A dual role for apolipoprotein e in neuroinflammation: anti- and pro-inflammatory activity. J. Mol. Neurosci. 23, 205–212.
Halim, A., et al., 2013. LC-MS/MS characterization of O-glycosylation sites and glycan structures of human cerebrospinal fluid glycoproteins. J. Proteome Res. 12, 573–584.
Hanson, A.J., et al., 2013. Effect of apolipoprotein E genotype and diet on apolipoprotein E lipidation and amyloid peptides: randomized clinical trial. JAMA Neurol. 70, 972–980.
Harris, F.M., et al., 2004. Astroglial regulation of apolipoprotein E expression in neuronal cells. Implications for Alzheimer's disease. J. Biol. Chem. 279, 3862–3868.
Hatters, D.M., et al., 2006. Apolipoprotein E structure: insights into function. Trends Biochem. Sci. 31, 445–454.
Hauser, P.S., et al., 2011. Apolipoprotein E: from lipid transport to neurobiology. Prog. Lipid Res. 50, 62–74.
Hayakawa, T., Varki, A., 2012. Human-specific changes in sialic acid biology. Post-Genome Biol. Prim. 123–148.
Heinsinger, N.M., et al., 2016. Apolipoprotein E genotype affects size of ApoE complexes in cerebrospinal fluid. J. Neuropathol. Exp. Neurol. 75, 918–924.
Hemonnot, A.-L., et al., 2019. Microglia in Alzheimer disease: well-known targets and new opportunities. Front. Aging Neurosci. 11.
Hu, J., et al., 2015. Opposing effects of viral mediated brain expression of apolipoprotein E2 (apoE2) and apoE4 on apoE lipidation and Aβ metabolism in apoE4-targeted replacement mice. Mol. Neurodegener. 10, 6.
Huang, Y., 2006. Apolipoprotein E and Alzheimer disease. Neurology. 66, S79–S85.
Huang, Y., Mahley, R.W., 2014. Apolipoprotein E: structure and function in lipid metabolism, neurobiology, and Alzheimer's diseases. Neurobiol. Dis. 72 (Pt A), 3–12.
Huang, Y., et al., 2004. Apolipoprotein E: diversity of cellular origins, structural and biophysical properties, and effects in Alzheimer's disease. J. Mol. Neurosci. 23, 189–204.
Huynh, T.V., et al., 2017. Apolipoprotein E and Alzheimer's disease: the influence of apolipoprotein E on amyloid-beta and other amyloidogenic proteins. J. Lipid Res. 58, 824–836.
Kara, E., et al., 2017. Isoform- and cell type-specific structure of apolipoprotein E lipoparticles as revealed by a novel Forster resonance energy transfer assay. J. Biol. Chem. 292, 14720–14729.
Kawasaki, K., et al., 2009. Sialic acid moiety of apolipoprotein E and its impact on the formation of lipoprotein particles in human cerebrospinal fluid. Clin. Chim. Acta 402, 61–66.
Keppler, O.T., et al., 1999. UDP-GlcNAc 2-epimerase: a regulator of cell surface sialylation. Science. 284, 1372–1376.
Kim, J., et al., 2009. The role of apolipoprotein E in Alzheimer's disease. Neuron. 63, 287–303.
Knoferle, J., et al., 2014. Apolipoprotein E4 produced in GABAergic interneurons causes learning and memory deficits in mice. J. Neurosci. 34, 14069–14078.
Kockx, M., et al., 2018. Cell-specific production, secretion, and function of apolipoprotein E. J. Mol. Med. (Berl). 96, 361–371.
Kuszczyk, M.A., et al., 2013. Blocking the interaction between apolipoprotein E and Aβ reduces intraneuronal accumulation of Aβ and inhibits synaptic degeneration. Am. J. Pathol. 182, 1750–1768.
LaDu, M.J., et al., 1994. Isoform-specific binding of apolipoprotein E to beta-amyloid. J. Biol. Chem. 269, 23403–23406.
Lee, Y., et al., 2010. Glycosylation and sialylation of macrophage-derived human apolipoprotein E analyzed by SDS-PAGE and mass spectrometry: evidence for a novel site of glycosylation on Ser290. Mol. Cell. Proteomics 9, 1968–1981.
Linnartz-Gerlach, B., et al., 2014. Siglec functions of microglia. Glycobiology. 24, 794–799.
Liu, C.C., et al., 2013. Apolipoprotein E and Alzheimer disease: risk, mechanisms and therapy. Nat. Rev. Neurol. 9, 106–118.
Liu, S., et al., 2017. Targeting apolipoprotein E/amyloid beta binding by peptoid CPO_Abeta17-21 P ameliorates Alzheimer's disease related pathology and cognitive decline. Sci. Rep. 7, 8009.
Mahley, R.W., 2016. Apolipoprotein E: from cardiovascular disease to neurodegenerative disorders. J. Mol. Med. (Berl). 94, 739–746.
Mahley, R.W., et al., 2009. Apolipoprotein E: structure determines function, from atherosclerosis to Alzheimer's disease to AIDS. J. Lipid Res. 50 (Suppl), S183–S188.
Manelli, A.M., et al., 2004. ApoE and Abeta1-42 interactions: effects of isoform and conformation on structure and function. J. Mol. Neurosci. 23, 235–246.
Matsubara, E., 2012. Lipoproteins and apolipoproteins in Alzheimer's disease. Lipoproteins - Role Health Dis.
Nielsen, H.M., et al., 2010. Astrocytic a beta 1-42 uptake is determined by A beta-aggregation state and the presence of amyloid-associated proteins. Glia. 58, 1235–1246.
Pankiewicz, J.E., et al., 2014. Blocking the apoE/Aβ interaction ameliorates Aβ-related pathology in APOE ε2 and ε4 targeted replacement Alzheimer model mice. Acta Neuropathol. Commun. 2, 75.
Perkins, M., et al., 2016. Altered energy metabolism pathways in the posterior cingulate in young adult apolipoprotein E ε4 carriers. J. Alzheimers Dis. 53, 95–106.
Rawal, P., Zhao, L., 2021. Sialometabolism in brain health and Alzheimer's disease. Front. Neurosci. 15, 648617.
Reiman, E.M., et al., 2004. Functional brain abnormalities in young adults at genetic risk for late-onset Alzheimer's dementia. Proc. Natl. Acad. Sci. U. S. A. 101, 284–289.
Sadowski, M., et al., 2004. A synthetic peptide blocking the apolipoprotein E/beta-amyloid binding mitigates beta-amyloid toxicity and fibril formation in vitro and reduces beta-amyloid plaques in transgenic mice. Am. J. Pathol. 165, 937–948.
Schedin-Weiss, S., et al., 2014. The role of protein glycosylation in Alzheimer disease. FEBS J. 281, 46–62.
Sierksma, A., et al., 2020. Novel Alzheimer risk genes determine the microglia response to amyloid-β but not to TAU pathology. EMBO Mol. Med. 12, e10606.
Stanley, P., 2011. Golgi glycosylation. Cold Spring Harb. Perspect. Biol. 3.
Strittmatter, W.J., et al., 1993. Binding of human apolipoprotein E to synthetic amyloid beta peptide: isoform-specific effects and implications for late-onset Alzheimer disease. Proc. Natl. Acad. Sci. U. S. A. 90, 8098–8102.
Tai, L.M., et al., 2013. Levels of soluble apolipoprotein E/amyloid-beta (Abeta) complex are reduced and oligomeric Abeta increased with APOE4 and Alzheimer disease in a transgenic mouse model and human samples. J. Biol. Chem. 288, 5914–5926.
Tai, L.M., et al., 2014. Soluble apoE/Abeta complex: mechanism and therapeutic target for APOE4-induced AD risk. Mol. Neurodegener. 9, 2.
Tesseur, I., et al., 2000. Prominent axonopathy and disruption of axonal transport in transgenic mice expressing human apolipoprotein E4 in neurons of brain and spinal cord. Am. J. Pathol. 157, 1495–1510.
Van Dooren, T., et al., 2006. Neuronal or glial expression of human apolipoprotein e4 affects parenchymal and vascular amyloid pathology differentially in different brain regions of double- and triple-transgenic mice. Am. J. Pathol. 168, 245–260.
Verghese, P.B., et al., 2013. ApoE influences amyloid-beta (Abeta) clearance despite minimal apoE/Abeta association in physiological conditions. Proc. Natl. Acad. Sci. U. S. A. 110, E1807–E1816.
Wightman, D.P., et al., 2020. Largest GWAS (N=1,126,563) of Alzheimer's disease implicates microglia and immune cells. medRxiv. 2020.11.20.20235275.
Wisniewski, T., Drummond, E., 2020. APOE-amyloid interaction: therapeutic targets. Neurobiol. Dis. 138, 104784.
Wu, L., Zhao, L., 2016. ApoE2 and Alzheimer's disease: time to take a closer look. Neural Regen. Res. 11, 412–413.
Wu, L., et al., 2018. Human ApoE isoforms differentially modulate brain glucose and ketone body metabolism: implications for Alzheimer's disease risk reduction and early intervention. J. Neurosci. 38, 6665–6681.
Xu, P.T., et al., 1999. Specific regional transcription of apolipoprotein E in human brain neurons. Am. J. Pathol. 154, 601–611.
Xu, Q., et al., 2006. Profile and regulation of apolipoprotein E (ApoE) expression in the CNS in mice with targeting of green fluorescent protein gene to the ApoE locus. J. Neurosci. 26, 4985–4994.
Xu, X., et al., 2017. Safety, pharmacokinetics and sialic acid production after oral administration of N-acetylmannosamine (ManNAc) to subjects with GNE myopathy. Mol. Genet. Metab. 122, 126–134.
Yoo, S.W., et al., 2015. Sialylation regulates brain structure and function. FASEB J. 29, 3040–3053.
Yu, J.T., et al., 2014. Apolipoprotein E in Alzheimer's disease: an update. Annu. Rev. Neurosci. 37, 79–100.
Zhong, N., Weisgraber, K.H., 2009. Understanding the association of apolipoprotein E4 with Alzheimer disease: clues from its structure. J. Biol. Chem. 284, 6027–6031.
Zhou, Z., et al., 1996. Alzheimer amyloid-beta peptide forms denaturant-resistant complex with type epsilon 3 but not type epsilon 4 isoform of native apolipoprotein E. Mol. Med. 2, 175–180.